Numerical Modeling of Cemented Mine Backfill Deposition

Matthew Helinski[1]; Martin Fahey[2]; and Andy Fourie[3]

Abstract: In current underground mining practice, it is common to use tailings, without added cement, to fill mined-out voids ("stopes"). If fine-grained tailings are used, the high placement rates and low permeability can often result in undrained loading conditions and, hence, lower effective stress, when assessed in the conventional manner. Where cement is added, the cement modifies the consolidation characteristics in a number of ways, including increasing the strength and stiffness, reducing the permeability, and inducing volumetric changes associated with the hydration reactions leading to "self-desiccation." As a result, conventional consolidation-analysis techniques are unsuitable for assessing the behavior. The one-dimensional mine-tailings-consolidation program (MinTaCo) has been modified, and renamed CeMinTaCo, to couple cement hydration with conventional consolidation analysis. The fundamental theory behind the modifications is presented. The model is used to undertake a sensitivity study, which highlights some of the important features of the behavior of cemented backfill, and shows how complex interactions between the various properties produce some outcomes that are counterintuitive.

DOI: 10.1061/(ASCE)1090-0241(2007)133:10(1308)

CE Database subject headings: Mining; Cements; Numerical models; Backfills.

Introduction

During the excavation of many underground ore bodies, the ore is extracted in large "blocks" known as "stopes." These stopes range in size but are generally of the order of 20 m × 20 m in plan area by 50 m high. After the ore has been extracted, the stope is refilled using a relatively dilute combination of tailings and water. The filling process is often quite rapid, in many cases over 10 m vertical rise per day (Le Roux 2004). In many cases, to achieve 100% ore extraction, these fill masses are exposed during the mining of adjacent stopes. In order to maintain stability in these circumstances, cement is often added to the mine tailings prior to placement. While the cement contents are often low (2%–10%), the volumes involved make this a major expense for most stoping operations. An illustration of the filling process is presented in Fig. 1.

Tunnels ("drives") connected to mine workings extend into these stopes and, in order to contain the backfill slurry from flowing into these tunnels, structural barricades are constructed at the head of the access tunnels. These are permeable, to allow the fill to drain. Between December 2003 and December 2004, there were reportedly at least seven slurry-fill barricade failures worldwide, with each of these failures resulting in an inrush of fill to the mine workings. Apart from the economic consequences of such failures, there is also great potential for injury or loss of life to miners located deeper in the mine at the time of the barricade failure.

The writers believe that many of these failures occur because existing design approaches for determining barricade loads are deficient in that they do not incorporate all the relevant mechanisms, such as consolidation and mechanisms associated with the cement-hydration processes (Rankin 2004; Kuganathan 2002). As demonstrated by Helinski et al. (2006), this behavior must be taken into account in a fully coupled way if the process is to be understood and if a reasonable estimate of barricade loads is to be obtained. It is believed that an improved understanding of the filling process (through coupled numerical modeling) will allow operators to more accurately predict barricade loads as well as provide direction for systems to manage the process.

This paper describes a preliminary version of a numerical model for simulating this process; it is preliminary in the sense that while it is fully coupled (coupling the effects of filling, consolidation, cement hydration, etc.), it is still only one-dimensional, and, as such, does not incorporate the effect of arching, which can have a major influence on stresses and pore pressures within a filled stope. While this is a significant deficiency in the preliminary model, the model nevertheless provides useful insights into the behavior of cemented backfill.

The paper commences with a brief overview of the original mine-tailings-consolidation (MinTaCo) model (Seneviratne et al. 1996) that formed the basis for the new model. The new model is then introduced, and the various modifications required to incorporate the additional effects due to cement hydration into the consolidation equations are explained. The model is then verified with some simple problems, and a sensitivity analysis is undertaken. To demonstrate the applicability of the model, an example is presented where modeling results are compared with results from in situ monitoring in an operational pastefill stope.

[1]Ph.D. Candidate, School of Civil and Resource Engineering, The Univ. of Western Australia, Perth, Australia. E-mail: helinski@civil.uwa.edu.au

[2]Professor, School of Civil and Resource Engineering, The Univ. of Western Australia, 35 Sterling Highway, Crawley, Perth, Australia (corresponding author). E-mail: fahey@civil.uwa.edu.au

[3]Professor, Australian Center for Geomechanics, The Univ. of Western Australia, Perth, Australia. E-mail:andyf@acg.uwa.edu.au

Note. Discussion open until March 1, 2008. Separate discussions must be submitted for individual papers. To extend the closing date by one month, a written request must be filed with the ASCE Managing Editor. The manuscript for this paper was submitted for review and possible publication on April 10, 2006; approved on March 14, 2007. This paper is part of the ***Journal of Geotechnical and Geoenvironmental Engineering***, Vol. 133, No. 10, October 1, 2007. ©ASCE, ISSN 1090-0241/2007/10-1308–1319/$25.00.

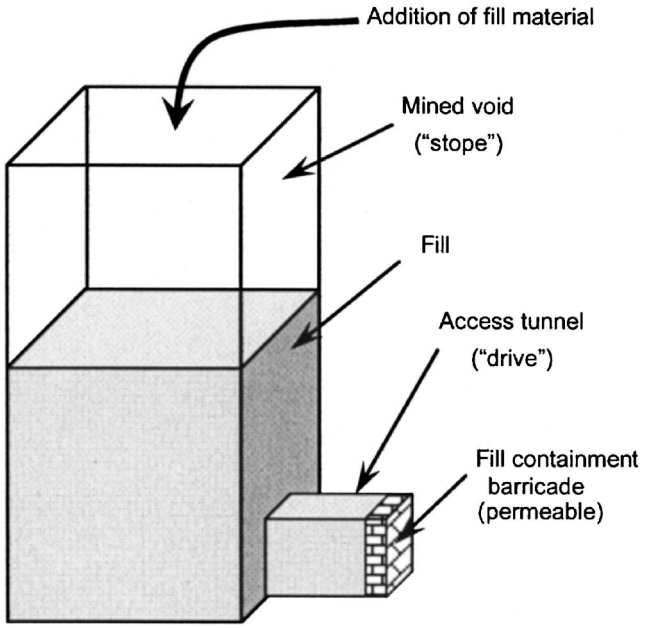

Fig. 1. Schematic drawing of a stope and access drive, and the stope backfilling process

Modeling the Behavior of Uncemented Tailings: MinTaCo Program

In previous work carried out over 10 years ago, the finite-element program, MinTaCo, was developed to model the consolidation and evaporation behavior of mine tailings, within the context of conventional tailings deposition in aboveground tailings storage facilities. A new program based on MinTaCo has been named "CeMinTaCo," to indicate that it deals with cemented-mine-tailings consolidation. A full description of the original MinTaCo is provided by Seneviratne et al. (1996). In brief, MinTaCo is a one-dimensional model, which uses a large-strain formulation with Lagrangian coordinates and Gibson's consolidation equations (Gibson et al. 1967) to deal with the large volume changes that occur as tailings consolidate from a slurry. The form of the Gibson one-dimensional consolidation equation is presented as Eq. (1)

$$\underset{\text{(A)}}{\frac{\delta u}{\delta t}} + \underset{\text{(D)}}{\left((1+e_o)\frac{\delta \sigma_v'}{\delta e}\right)}\left\{\frac{\delta}{\delta a}\left[\underset{\text{(C)}}{\frac{k}{\gamma_w}\left(\frac{1+e_o}{1+e}\right)}\frac{\delta u}{\delta a}\right] + \frac{\delta k}{\delta a}\right\} = \underset{\text{(B)}}{\frac{\delta \sigma_v}{\delta t}} \quad (1)$$

where a=a Lagrangian coordinate, u=pore pressure, k=hydraulic conductivity (permeability), e=void ratio, and σ_v' and σ_v=vertical effective and total stresses, respectively. In this equation, term A=rate of change in pore pressure as a result of a rate of application of total stress (term B), term C=volumetric strain, which is controlled by the permeability (k) of the material and the hydraulic gradient ($\delta u/\delta a$), and term D describes the current stiffness of the material.

The large volume changes that occur as tailings consolidate required the incorporation of nonlinear $k-e$ (permeability–void ratio) and $e-\sigma_v'$ (void ratio–effective stress) relationships, expressed using power functions suggested by Carrier et al. (1983)

$$e = a_c(\sigma_v')^{b_c}$$

$$k = \frac{c_k(e)^{d_k}}{1+e} \quad (2)$$

where a_c and b_c=soil-compression constants (with values depending on the units of σ_v'), and c_k and d_k=permeability constants (the former having the same dimensions as k).

The MinTaCo program was developed to deal with staged filling of tailings storage areas, with particular reference to practice in Australia. As such, it incorporated features such as being able to add fresh tailings slurry at any desired rate, which may be changed over time, variable base-drainage conditions, and a method of incorporating the effect of surface evaporation. Since its development, it has been used extensively for modeling a wide variety of tailings filling operations (see, for example, Fahey and Newson 1997; and Fahey et al. 2002).

Modeling the Behavior of Cemented Tailings: CeMinTaCo Program

During the consolidation of uncemented mine tailings from an initial slurry state, both the stiffness (compressibility) and the permeability of the material change as the void ratio reduces, as defined by Eq. (2). When cement is added, these changes still occur, but a number of other mechanisms associated with cement hydration are introduced, which also need to be addressed in the model:

- The stiffness increases as a result of void-ratio reduction, but also as a result of the gradual formation of cement bonds during hydration. These bonds may be damaged by ongoing compression, even as they form. These additional factors require modification of the compressibility term in Eq. (1) (term D);
- The permeability is still a function of void ratio, but it is also affected by the growth of cement gel in the voids. This requires modification of the permeability term in Eq. (1) (term C);
- The large increase in stiffness of the cementing soil matrix results eventually in the matrix bulk stiffness being comparable to that of water, which must be taken into account in determining pore-pressure response to change in total vertical stress (term A); and
- In cemented tailings, the volume of hydrated cement is less than the combined volume of the unhydrated cement and the water used in hydration—effectively, volume is "consumed" in the hydration process. This "self-desiccation" process functions like an internal water "sink," which can cause a significant change in pore pressure. This requires development of an additional term in Eq. (1).

A new consolidation equation incorporating these changes is presented as Eq. (3)

$$\underset{\text{(A)}}{\left[\frac{\delta u}{\delta t}\left(\frac{K_w}{E_o'+K_w}\right) + \frac{\delta \sigma_v'}{\delta t}\left(\frac{(1+e)E_o'}{E_o'+K_w}\right)\right]} + \underset{\text{(D)}}{\left((1+e_o)\frac{\delta \sigma_v'}{\delta e}(e, C_c, t^*, \sigma_v')\right)} \times \left\{\frac{\delta}{\delta a}\left[\underset{\text{(C)}}{\frac{k(e_{\text{eff}})}{\gamma_w}\left(\frac{1+e_o}{1+e}\right)}\frac{\delta u}{\delta a}\right] + \frac{\delta k(e_{\text{eff}})}{\delta a}\right\} + \left[(1+e_o)\frac{\delta \sigma_v'}{\delta a}\underset{\text{(E)}}{\left(-\frac{\delta V_{hyd}}{\delta t}\right)}\frac{\delta \sigma_v'}{\delta e}\cdot\left(\frac{3(1-\upsilon)}{1+\upsilon}\right)\right] = \underset{\text{(B)}}{\frac{\delta \sigma_v}{\delta t}} \quad (3)$$

In this equation, the modified terms are identified using the same labels as the equivalent unmodified terms in Eq. (1). The term dealing with the effect of self-desiccation (term E) is an extra term, which does not have an equivalent in the unmodified equation.

In the following subsections, the basis for each of these modifications is explained in turn, and all the new parameters in the equation are defined. At the same time, the basis of the methods proposed for determining the values of the parameters is provided, and some experimental results are presented to show the applicability of the relationships derived.

Compressibility and General Stress–Strain Behavior

Modeling the evolving stiffness of a material undergoing cementing is complex, since during the hydration process the behavior gradually changes from that of an uncemented material to that of a fully cemented material. It is therefore necessary to consider the whole (compressive) stress–strain response of the material at all stages of the process, including the evolution of initial yield stress and ultimate strength, and the evolution of small-strain stiffness. As will be shown, a key assumption is that stiffness, yield stress, and ultimate strength evolve in a similar manner, and the rate of evolution of any one of these parameters can be used to estimate the rate of evolution of any of the others.

Hardening and Damage

To incorporate the effect of cementation on strength and stiffness, a convenient starting point is the structured cam clay model developed by Liu and coworkers at Sydney University (Liu et al. 1998; Liu and Carter 2002; and Carter and Liu 2005). In this approach, "structure" (which could include cementation) has the effect of increasing the isotropic (or one-dimensional) compression yield stress in a manner analogous to overconsolidation. Thus, in the case of cemented mine backfill, the yield stress in isotropic compression (p'_y) is a function of void ratio and cementation, and, hence, it changes over time due to both of these changing over time. Therefore, a considerable extension to the structured cam clay model is required in this case to deal with the combined effects of growth of structure as hydration occurs, and possible damage to this structure due to yielding with increasing effective stress.

The original MinTaCo program incorporated a power-law relationship to deal with the changing compressibility and permeability with ongoing compression for an uncemented material [Eq. (2)]. To allow for a more consistent framework within the new model, the power function relationship for compression ($e-\sigma'_v$) in Eq. (2) has been changed to the conventional cam clay relationship

$$\Delta e = -\lambda \cdot \ln\left(\frac{\sigma'_v + \Delta\sigma'_v}{\sigma'_v}\right) \tag{4}$$

$$\Delta e = -\kappa \cdot \ln\left(\frac{\sigma'_v + \Delta\sigma'_v}{\sigma'_v}\right) \tag{5}$$

where Δe=the change void ratio in the current time increment; λ and κ=conventional cam clay compressibility parameters; σ'_v=current vertical effective stress; and $\Delta\sigma'_v$=vertical effective-stress increment. The "normally consolidated" relationship [Eq. (4)] applies to loading of the material on the uncemented compression line, while the elastic compression relationship [Eq. (5)] applies to material undergoing compression (or swelling) at stress levels below the uncemented compression line.

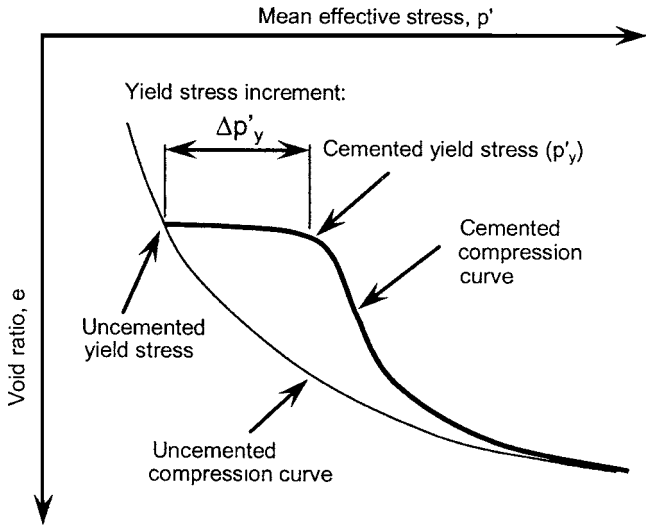

Fig. 2. Isotropic compression curves for cemented and uncemented material

The principle that has been adopted to determine the cement contribution to compression resistance follows the concept suggested by Rotta et al. (2003). They proposed the concept of an isotropic yield-stress increment ($\Delta p'_y$) and define this as being the difference between the primary yield stress and the (effective) stress applied during curing. Because mine-fill material is generally placed and consolidated along the normally consolidated line, it is assumed here that the curing stress corresponds to the yield stress of the material in an uncemented state. Therefore, $\Delta p'_y$ is taken to represent the difference between the yield stresses for the cemented and uncemented material and at the same void ratio. The concept is illustrated in Fig. 2, which presents a schematic plot of mean effective stress (p') versus void ratio (e) for soil in uncemented and cemented states during isotropic compression.

Rotta et al. (2003) suggested that $\Delta p'_y$ is a measure of the bond strength, and Consoli et al. (2006) extended this concept to show that $\Delta p'_y$ is proportional to unconfined compressive strength (q_u). From this, it is considered reasonable to assume that this proportionality would also apply for one-dimensional compression, where the vertical yield-stress increment ($\Delta\sigma'_{vy}$) is defined similarly to $\Delta p'_y$. Therefore, the yield stress for a cemented soil in one-dimensional compression (σ'_{vy}) has been assumed to be the sum of the yield stress for the uncemented material and the yield-stress increment $\Delta\sigma'_{vy}$. Furthermore, based on the findings of Consoli et al. (2006), it has been assumed that $\Delta\sigma'_{vy}$ can be linearly related to q_u.

During the filling process, previously placed fill is subjected to mechanical processes that cause changes to the yield stress (σ'_{vy}). These include:

- Conventional soil hardening due to void-ratio reduction (dH);
- Increases in yield stress with time due to cementation (dHyd); and
- A potential reduction in strength due to plastic deformation—effectively, yielding of the cement bonds as compression occurs simultaneously with hydration (dD).

The effects of each of these are superimposed, to obtain the overall hardening rate:

$$\frac{d\sigma'_{vy}}{dt} = \frac{dH + dHyd - dD}{dt} \tag{6}$$

The conventional soil strain-hardening term (dH) is a function of the uncemented soil properties λ, κ, and Γ

$$dH = \exp\left(\frac{\Gamma - \Delta e^p}{\lambda - \kappa}\right) \tag{7}$$

where λ and κ are as defined earlier; Γ=the void ratio on the normal consolidation line, an effective stress of 1 kPa; and Δe^p=the plastic component of the change in void ratio.

The additional hardening that occurs due to cement hydration (dH_{yd}) is obviously a function of cement content and the time from the start of hydration. However, it has been well documented (e.g., Leroueil and Vaughan 1990; Consoli et al. 2000; Li and Aubertin 2003; Rotta et al. 2003) that the density (or void ratio) of the soil at the start of and during hydration is also an important factor. Rotta et al. (2003) developed an empirical equation to relate the isotropic yield-stress increment ($\Delta p'_y$) to cement content and void ratio (e), and a slightly modified version of this equation has been adopted here

$$\Delta p'_y = A \cdot \exp\left(\frac{X \cdot C_c + C_c^{0.1} - e}{Z \cdot C_c + W}\right) \tag{8}$$

where C_c is cement content (weight of cement per unit weight of solids); X, W, and Z are dimensionless constants; and A is a constant with the same units as $\Delta p'_y$.

Assuming that $\Delta\sigma'_{vy}$, q_u, and $\Delta p'_y$ are all proportional, data from either an isotorpic or a one-dimensional compression test may be used to derive the constant terms (A, X, Z, and W). An example of this is given in Figs. 3(a and b), which show Eq. (8) fitted to unconfined compression test data (q_u) for CSA hydraulic fill and Cannington paste-fill data (Rankin 2004), respectively, indicating that this equation can appropriately describe the cementation strength in typical cemented mine-backfill material. For one-dimensional compression analysis, the most direct method of determining all constants (A, X, W, and Z) is through regression analysis on a series of one-dimensional compression tests.

The "maturity relationship" that has been adopted to represent the progress of hydration over time is an exponential relationship originally presented by Rastrup (1956) and republished by Illston et al. (1979)

$$m = \exp\left(\frac{-d}{\sqrt{t - t_o}}\right) = \exp\left(\frac{-d}{\sqrt{t^*}}\right) \tag{9}$$

where m=the degree of maturity (representing the normalized value of a parameter, which is 0 at the start of the process and 1 at the end); d=a maturity constant (with units of time$^{1/2}$); t=the total elapsed time; and t_o=the time at initial set (and, hence, t^*=time after initial set).

A series of unconfined compression tests was carried out at different stages of hydration to assess the application of Eq. (9) to the development of q_u over time. Fig. 4 shows the results as normalized q_u (i.e., $q_u/q_{u\text{-max}}$) plotted against time for both Cannington paste fill (PF) (Rankin 2004) and CSA hydraulic fill (HF). Based on regression of the two data sets in Fig. 4, maturity constants (d) of 2.6 day$^{1/2}$ and 0.9 day$^{1/2}$ provided a reasonable match to the PF and HF, respectively, with the duration until initial set (t_o) being 0.16 days (~3.8 h) for each case.

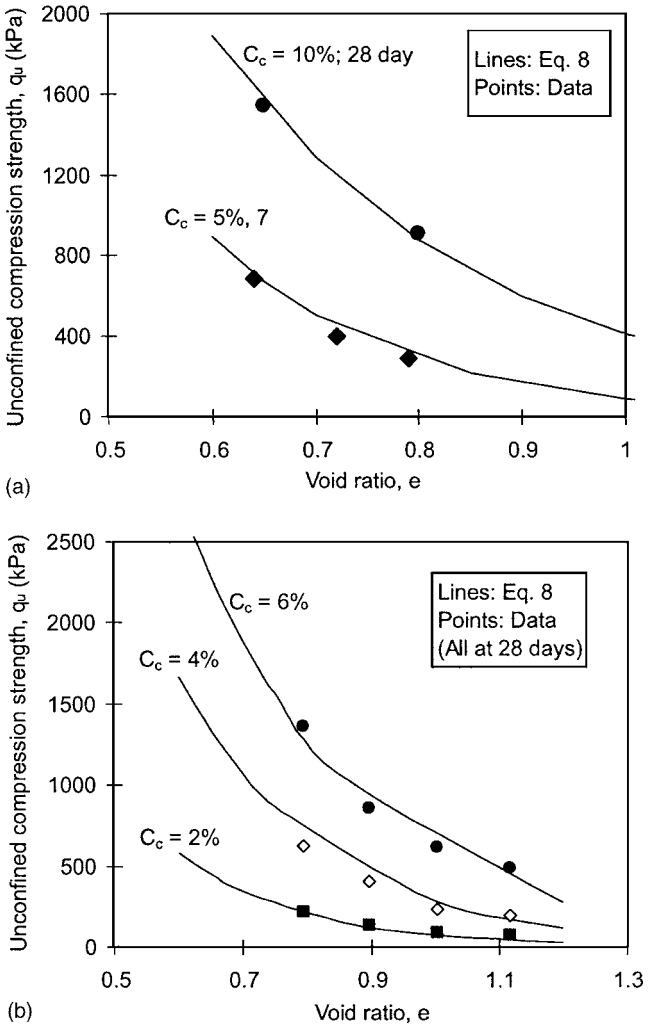

Fig. 3. Empirical fit of Eq. (8) to q_u data from (a) CSA hydraulic fill; (b) Cannington paste fill (C_c is cement content)

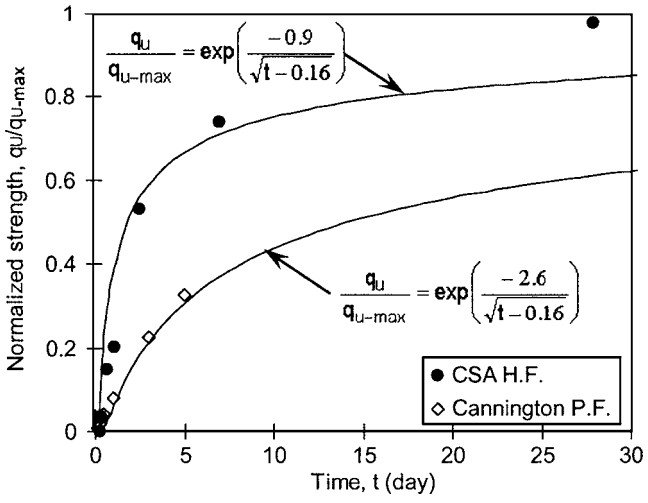

Fig. 4. Normalized strength ($q_u/q_{u\text{-max}}$) for two fill materials, and fitted relationships

Equation (9) may be combined with the yield-stress-increment relationship [Eq. (8)] to determine the increase in bond strength (dHyd) in time increment Δt

$$\mathrm{d}Hyd = \left[\exp\left(\frac{-d}{\sqrt{t^* + \Delta t}} \right) - \exp\left(\frac{-d}{\sqrt{t^*}} \right) \right] A \exp\left(\frac{X \cdot C_c + C_c^{0.1} - e}{Z \cdot C_c + W} \right) \tag{10}$$

It should be noted that the change in bond strength is incremented in accordance with the material state at t_o, the time at the start of hydration. This ensures than any strain hardening of the soil matrix due to consolidation that occurs prior to hydration is accounted for when evaluating hardening due to hydration.

As hydration may be occurring simultaneously with an increase in effectives stress (due to consolidation and/or due to the self-desiccation mechanism discussed later) the newly forming structure may experience damage due to the evolving yield stress being exceeded. This damage may occur as a result of loading within the yield surface (subyielding) as well as loading outside the yield surface (virgin yielding).

The damage relationship adopted here follows the approach used in the structured cam clay model (Liu et al. 1998; Liu and Carter 2002; Carter and Liu 2005). In this approach, incremental plastic volumetric strain induces damage, which is manifest as a reduction in the size of the yield surface. The function adopted to account for plastic volumetric strain in the model follows the work of Carter and Liu (2005), where the plastic component of strain may be represented by

$$\mathrm{d}\varepsilon_v^p = \left(1 - \frac{\eta}{M^*} \right) \left(\frac{\alpha(\lambda^* - \kappa^*)\mathrm{d}p' + \alpha^3 b|\mathrm{d}p'|}{(1+e)p_y'} \right) \tag{11}$$

where the asterisk (*) in this case indicates uncemented properties; η=the stress ratio (q/p'), M=the stress ratio at critical state, p'=the applied mean effective stress, p_y'=the yield stress, b=a constant representing the rate of structural breakdown, and

$$\alpha = \left(\frac{p' - p_u'}{p_y' - p_u'} \right) \tag{12}$$

where p_u'=stress at which kinematic hardening or destruction occurs (this subyielding function allows progressive destruction of bonds prior to reaching the yield stress).

Given the plastic strain increment, the damage dD (the reduction in compressive yield stress p_y') may be determined as

$$\mathrm{d}D = \frac{(1+e)bp_y'|\mathrm{d}\varepsilon_v^p|}{(\lambda^* - \kappa^*)\left\{ 1 + b\left[\ln\left(\frac{p_y'}{p_o'} \right) - c \right] \right\}} \left[\ln\left(\frac{p_y'}{p_o'} \right) - c \right] \tag{13}$$

where p_o'=the stress on the normal consolidation line for an uncemented soil at the same void ratio and c=a constant (the void ratio separating the limiting compression lines of the cemented and uncemented soils). For the very low cement contents commonly used in cemented mine fill, the term c would be equal to zero, since the assumption in this case is that the limiting compression lines coincide, as illustrated in Fig. 2.

A common approach used to simplify one-dimensional consolidation problems is to derive compression parameters required for the analysis using one-dimensional compression tests. This simplification allows all calculations to be carried out in terms of vertical effective stress (σ_v') rather than mean and deviator stresses (p' and q). While changes in Poisson's ratio (due to cementation) modify the stress path in one-dimensional compression, a simplification adopted for the present into CeMinTaCo is to replace all p' terms in Eqs. (12)–(14) by equivalent σ_v' terms, and set the stress ratio term (η) to zero.

Stiffness

The previous sections addressed the change in yield stress due to strain hardening, cement hydration, and damage. These processes also influence the material stiffness, and in order to undertake consolidation analysis it is therefore essential to characterize the material stiffness changes that occur. In an approach similar to that used for characterizing the evolution of one-dimensional yield stress, σ_{vy}', it is assumed that the stiffness of the cemented soil is a combination of the stiffness due to the uncemented soil skeleton and that due to the cementation. The uncemented stiffness is determined in accordance with Eqs. (4) and (5), while the additional cemented component is assumed to be proportional to the cemented component of strength ($\Delta\sigma_{vy}'$, q_u, or $\Delta p_y'$).

A series of experiments was carried out to assess the validity of this assumption. These experiments involved the measurement of small strain-shear stiffness (G_o or $G_{\max}$) using bender elements (Dyvik and Olsen 1989), prior to unconfined compression testing of these specimens. The bender element technique involves generating a shear wave at the top of a sample using a piezoceramic "bender element," and picking up the arrival of that shear wave at the other end using a similar bender element.

Fig. 5(a) shows the values $G_{o(\mathrm{inc})}$ plotted against q_u for a variety of combinations of CSA hydraulic fill mixes, where $G_{o(\mathrm{inc})}$=increase in G_o above the uncemented value. Similarly, Fig. 5(b) shows the relationship between Young's modulus and q_u for Cannington paste fill as in Rankin (2004). These plots indicate that for a range of material strengths and material types, there appears to be a reasonably linear correlation between the cement component of stiffness and cemented strength (q_u). Therefore, if $\Delta\sigma_{vy}'$ or q_u are known, it is reasonable to assume that a constant of proportionality may be applied to calculate the cement component of the stiffness. These Young's modulus or shear modulus values can be converted to constrained modulus (E_o') values using Poisson's ratio, and these may be combined with the constrained modulus values for uncemented soil to give total values of constrained modulus for every stage of hydration.

Having presented the details of how the various constitutive aspects are related in order to characterize the mechanical response of the cemented mine tailings during filling, these aspects can be combined so that the stiffness terms in Eq. (3) can be determined as a function of material density (i.e., void ratio, e), cement content (C_c), time from the start of hydration (t^*), and effective stress (σ_v')

$$E_o' = (1+e_o)\frac{\delta\sigma_v'}{\delta e} = f(e, C_c, t^*, \sigma_v') \tag{14}$$

Permeability

In the MinTaCo model, it was assumed that the permeability of the material varies as a function of void ratio, as expressed in Eq. (2). This $k-e$ relationship has been maintained in the CeMinTaCo model, but an "effective" void ratio term, e_{eff}, has been substituted for the e term to account for the effect on permeability of growth of cement gel in the voids. The basis of this is as follows.

The hydration of cement is associated with a growth of cement

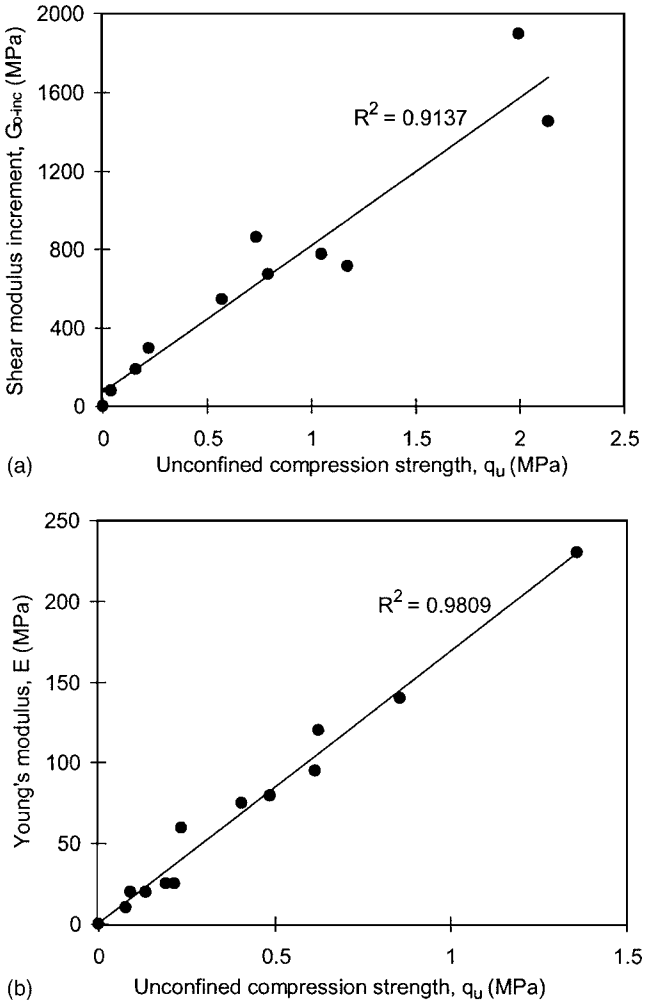

Fig. 5. Relationship between (a) $G_{o(\text{inc})}$ and q_u for CSA hydraulic fill; (b) between Young's modulus and q_u for Cannington paste fill

products, in the form of solid-cement hydrates as well as cement gel, which fill some of the void volume. These contribute to a reduction in permeability—the cement hydrates because of their very low permeability, and the cement gel because of its relatively low permeability. Illston et al. (1979) suggest that when combined with water, the solids and gel volume created (after full hydration) is about 80% greater than the initial unhydrated cement volume.

In order to account for this behavior, the permeability relationship in Eq. (2) has been modified to be in terms of effective void ratio, e_{eff}, which is calculated taking into account the void-ratio prior to hydration and the void-space infilling resulting from growth of hydrating-cement products

$$k = \frac{c_k(e_{\text{eff}})^{d_k}}{(1+e)} \tag{15}$$

where

$$e_{\text{eff}} = f(e, C_c, t^*) \tag{16}$$

As with other properties, the rate at which the growth of cement products takes place is simulated using the maturity relationship [Eq. (9)], and this combines with the change in void ratio due to compression to give the e_{eff} term in Eq. (15).

Pore-Pressure Change due to Change in Total Stress

The consolidation equation for uncemented material [Eq. (1)] is based on the assumption that, because of the low stiffness of the soil "skeleton" relative to that of water, an increase in σ_v due to the application of a new layer results in an equal increase in u and, hence, creates no immediate change in σ'_v. However, when cement is added, the stiffness of the cemented material can approach that of water as hydration nears completion, and thus an increase in σ_v at this stage results in an increase in σ'_v as well as an increase in u. Based on the requirement for strain compatibility, the distribution of σ_v between the soil effective stress (σ'_v) and the pore pressure (u) is proportional to the constrained modulus of the soil skeleton (E'_o) relative to the bulk stiffness of the pore water (K_w)

$$\frac{\delta\sigma_v}{\delta t} = \frac{\delta p \cdot K_w}{\delta t(E'_o + K_w)} + \frac{\delta\sigma'_v \cdot (1+e)E'_o}{\delta t(E'_o + K_w)} \tag{17}$$

This is incorporated into the modified term A in Eq. (3).

Self-Desiccation

The term labeled E in Eq. (3), which does not have any equivalent in Eq. (1), relates to the so-called self-desiccation mechanism and its potential effect on pore pressure. This term is reproduced here

$$\frac{\delta}{\delta a}(1+e_o)\left(-\frac{\delta V_{\text{hyd}}}{\delta t}\right)\frac{\delta\sigma'_v}{\delta e}\left(\frac{3(1-v)}{1+v}\right) \tag{18}$$

where $\delta V_{\text{hyd}}/\delta t$=rate of net water volume reduction in the hydration process. As already mentioned, self-desiccation is the process whereby the chemical reactions associated with cement hydration create an overall reduction in volume—i.e., the volume of the hydrated cement particles is less than the combined volume of the unhydrated cement particles and the water used in hydration. This volume reduction allows some "relaxation" of the pore water, which can result in a pore-pressure reduction.

Helinski et al. (2007) showed that the rate of net water volume consumption at any time after the start of hydration (t^*) may be calculated as

$$\frac{\delta V_{\text{hyd}}}{\delta t} = 0.5E_h w_c d(t^*)^{-1.5}\exp\left(\frac{-d}{\sqrt{t^*}}\right) \tag{19}$$

where d=maturity coefficient, E_h=efficiency of hydration factor (both dimensionless parameters), and w_c=weight of cement contained in each element.

The volumetric changes due to self-desiccation are entirely dependent on the chemical reactions that take place. Powers and Brownyard (1947) suggest that E_h is in the order of 6.4% for general Portland cement paste. However, the reactions that take place are highly dependent on the cement type, tailings mineralogy, and the chemicals remaining in the tailings after the completion of ore processing. Therefore, it is expected that both the maturity (d) and efficiency (E_h) terms vary for different cement-tailings combinations, but for any particular cement-tailings combination, testwork to date indicates that d and E_h are constant, regardless of C_c.

Helinski et al. (2007) discuss this self-desiccation concept with respect to cemented backfill, and provide an analytical solution for the change in pore pressure as a function of soil stiffness, water stiffness, and density for an undrained situation. In addition, they present an experimental method whereby this analytical solution can be used to interpret experimental results relating to the

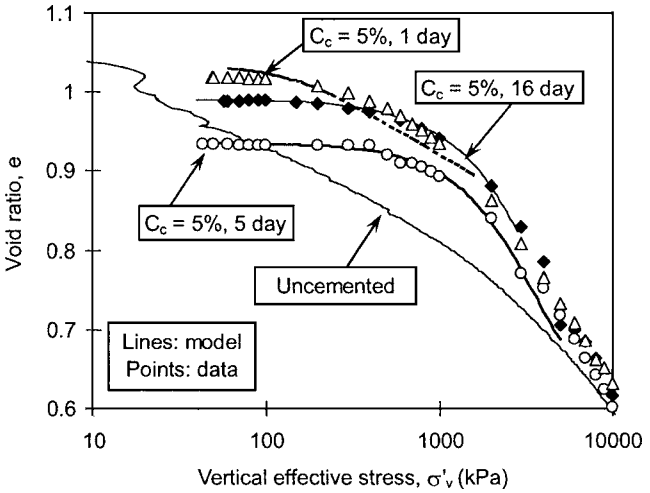

Fig. 6. Comparison of the proposed constitutive relationship with experimental results for one-dimensional compression (for cemented samples, legend shows the cement content and curing time in days)

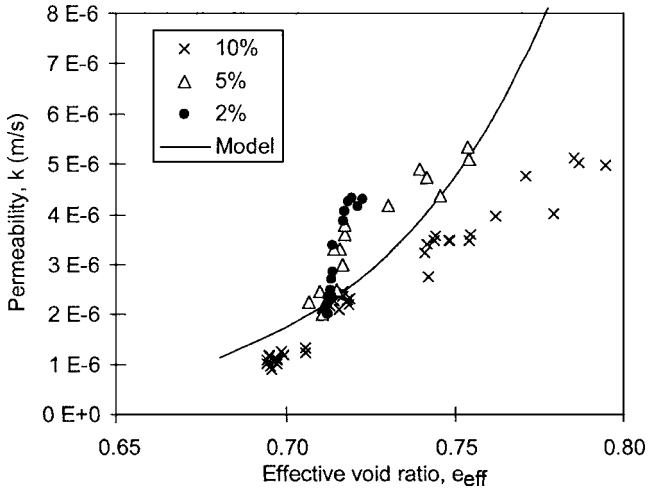

Fig. 7. Comparison of permeability model with experimental data

measured reduction in pore pressure and the measured small strain stiffness in order to determine both E_h and d.

Experimental Verification

It has already been shown that various components of the model can fit experimental data quite well. Thus, Fig. 4 showed it can give a good fit to the form of the strength gain over time, and other assumptions in the model have also been shown to be reasonable. In this section, some other verification experiments are described, relating to the aspects of overall compression behavior, permeability change, and the self-desiccation mechanism.

Compressibility

In order to demonstrate its applicability in modeling the compressibility, the proposed approach has been used to simulate a series of one-dimensional compression tests on cemented CSA hydraulic fill, in which the specimens were prepared at different densities and allowed to cure for different times prior to loading. The material constants d, X, W, and Z [in Eq. (10)] were determined from the measured values of q_u and from G_o values obtained from bender elements. The parameters λ^* and κ^* [in Eq. (13)] were determined from one-dimensional compression tests on uncemented material, and through modifying terms A [in Eq. (10)] and b [in Eq. (13)], the one-dimensional compression response could be adequately represented, as shown in Fig. 6. This indicates that, given a suitable suite of experimental results, the proposed constitutive relationship provides a good representation of the behavior of material undergoing curing, compression, and cementation breakdown.

Permeability

In order to test the overall approach to estimating permeability embodied in Eq. (15) [and (16)], a series of permeability experiments was conducted in a triaxial cell, where the cell pressure and back pressure were maintained at 520 kPa and 500 kPa, respectively, to maintain full saturation. As curing progressed, permeability measurements were taken at regular intervals. This involved changing the back pressure at the top boundary to 510 kPa, and that at the base to 490 kPa, thereby establishing a hydraulic gradient of about 13 across the 150-mm-long sample, and measuring the resulting steady-state flow rate. At the completion of the test, the sample dimensions were measured and, based on the initial dry weight, the void ratio could be calculated. The results of tests on cemented hydraulic fill with cement contents (C_c) of 2%, 5%, and 10% are presented in Fig. 7, which shows the measured values of k plotted against the calculated values of e_{eff} for the different experiments. The model estimate is also shown (the solid line), where the same value for d is used as for the other relationships (i.e., d=0.9).

It should be noted that working out e_{eff} for each measured value of k is based on the assumption that the final volume of the cement products in the pores can be calculated from cement behavior principles, and that during hydration, the growth in the cement-product volume follows the same form as all the other relationships (i.e., strength, stiffness, etc.). Given the uncertainty around this assumption, the agreement (or lack thereof) between the model estimate and the measured values is acceptable at this stage, though it is clear that further refinement of this aspect is required.

Self-Desiccation

In order to verify the self-desiccation aspect of the model, an undrained self-desiccation test was carried out, and the CeMinTaCo program was used to reproduce the behavior observed in the test. The test involved preparing a fully saturated sample of CSA hydraulic fill, at a void ratio of 0.7 and cement content of 5%, in the form of a triaxial test sample. This was mounted in a triaxial cell, and enclosed in a latex membrane in the usual way. The sample was subjected to a total cell pressure of 850 and an initial back pressure of 830 kPa. Then, the back-pressure valve was closed, so that the hydration process could take place in a completely undrained state. A full description of the test procedure is provided in Helinski et al. (2007).

The results are shown in Fig. 8 as a plot of measured pore pressure versus time. In this case, the self-desiccation mechanism has reduced the pore pressure from the initial back pressure value of 830 kPa to a final value close to zero. (This suggests that it might have been appropriate to start from an even higher back pressure in this case, to ensure a final pore pressure well above

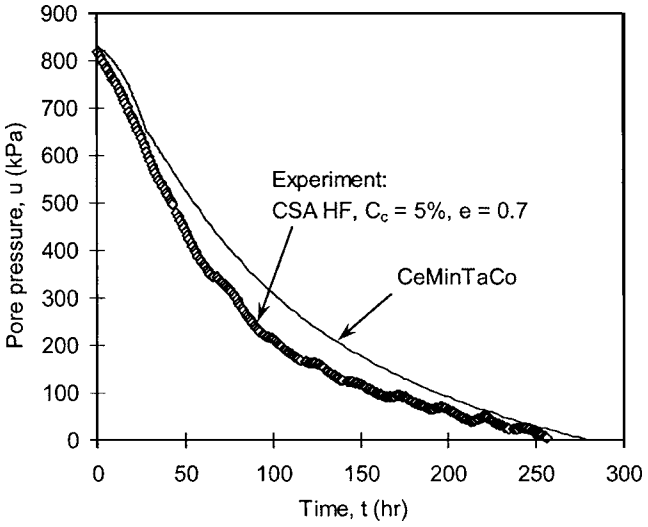

Fig. 8. Comparison of undrained self-desiccation test and CeMinTaCo prediction of pore-pressure (u) reduction against time

Table 1. Base-Case Material Properties

Property	Value adopted
Placement void ratio (e)	1.0
Cam-clay friction term (M)	1.0
Swelling/recompression coefficient (κ)	0.006
Virgin compression coefficient (λ)	0.06
Void ratio at $\sigma'_v = 1$ kPa on the normal consolidation line (Γ)	1.3
Permeability parameters in Eq. (15) (c_k: m/day; d)	0.0024, 20
Soil-particle specific gravity (G_s)	2.72
Cement content (C_c: %)	0 and 5
Damage coefficient (b)	0.5
Constant A in Eq. (8) (kPa)	7
$\Delta\sigma'_{vy}/q_u$	6
E'_o/q_u	2000
Maturity term (d: day$^{1/2}$)	0.9
Time until initial set (t_o: day)	0.167
Efficiency of hydration (E_h: cm^3/g)	0.032

zero.) The response fitted using the CeMinTaCo program is also shown in Fig. 8, which indicates that the program is capable of reproducing the observed experimental results quite well. This experiment shows how effective the self-desiccation mechanism can be in reducing pore pressure (and, hence, in increasing effective stress). In this case, this occurs in the absence of any external drainage effects, but in a real stope, it would combine with any "consolidation drainage" to produce much faster pore-pressure reduction than would otherwise be the case.

Sensitivity Study

This section describes a limited sensitivity study undertaken to illustrate the effect of varying some of the input parameters on the overall response predicted in modeling the filling of a typical stope. The filling strategy used in the study was based on typical filling practice (in Australia), and involved filling an initial "plug" at 0.4 m/h for 16 h, followed by a 24-h rest period, and then completing filling the remaining 30 m at a rate of 0.4 m/h. The base case set of input parameters used in the study is given in Table 1, and, except where otherwise indicated, these parameters are used in all the examples that follow.

It should be noted that while the model appears to require a large number of input parameters, the information can often be generated using a modest set of laboratory experiments. These would typically include an undrained self-desiccation test (as described above), a limited series of unconfined compression tests (on the self-desiccation test sample), and one-dimensional compression tests.

Proper simulation of the three-dimensional (3D) geometry of a real stope and permeable drawpoint (illustrated in Fig. 1) would require a 3D FE program, or at least a two-dimensional or axisymmetric program. However, since the version of CeMinTaCo presented here is only one-dimensional, a means of simulating the restriction to drainage resulting from the reduced drawpoint cross section was required. The method adopted is illustrated in Fig. 9, which consisted of introducing a 5-m-thick layer with reduced permeability (one-eighth of the value adopted for the bulk of the material at a corresponding void ratio) at the base of the stope. Note, however, that the material in this region had zero cement content, so none of the effects of self-desiccation apply in this region. In the following sections, the effect of changing a number of parameters is investigated.

Influence of Cementation

To illustrate the effect of cementation on the consolidation response, analysis was first carried out using uncemented material. Then, the analysis was repeated twice with cement content (C_c) of 5%, in one case with the self-desiccation mechanism disabled in the model, and the other with it enabled. Fig. 10 presents the results of these analyses as plots of pore pressure (2 m above the base drainage layer) versus time. Also shown is a plot of the total vertical stress versus time at the same point in the profile. These plots indicate that for the case without any cement, the increase in pore pressure is similar to the increase in total stress, and, hence, very little effective stress is generated during filling. After the

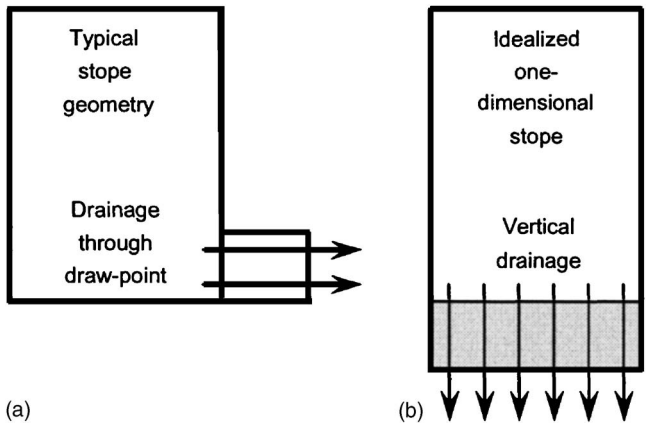

Fig. 9. Idealization of base-drainage conditions for consolidation modeling: Drainage restriction due to reduced area of drawpoint (a); idealization of this restriction in the CeMinTaCo modeling (b). The permeability of the shaded area is about one-eighth of that of the rest of the material.

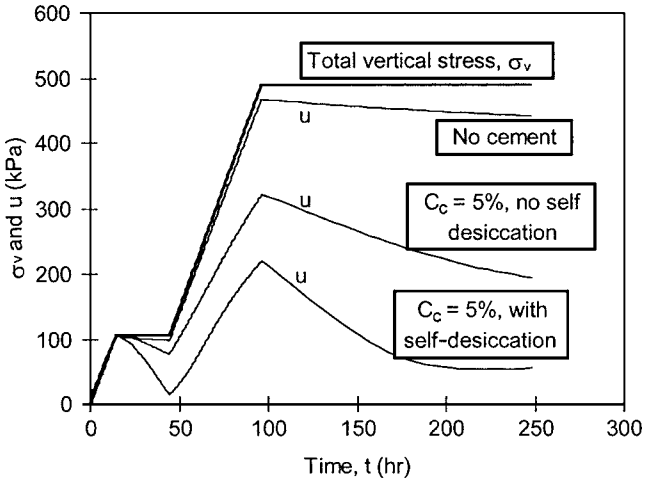

Fig. 10. Effect of cement content and self-desiccation on pore pressures during and following filling of a stope (for a point 7 m above the base of the stope)

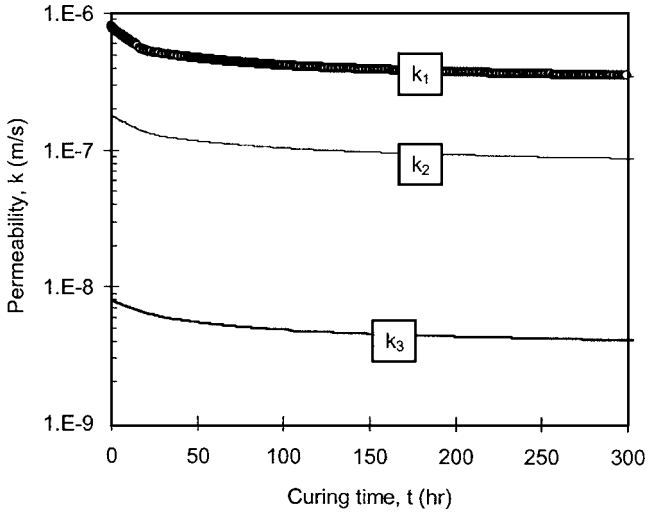

Fig. 11. Three permeability relationships adopted in the permeability sensitivity study

completion of filling, the rate of dissipation of pore pressure is slow, and very little consolidation has occurred at the end of the period modeled (250 h).

For the second case, it may be seen from Fig. 10 that, even with the self-desiccation mechanism disabled, pore pressures after hydration starts are significantly less than for the uncemented case. The added cement produces an increase in soil stiffness (after the start of hydration) and a reduction in permeability, as previously discussed. Since the rate of pore pressure reduction (consolidation) is dictated by the product of stiffness and permeability, this result indicates that in this case the increase in stiffness outweighs the reduction in permeability, and, hence, more dissipation occurs, even during filling. However, it should be noted that there are still significant excess pore pressures present at the end of filling, but due to the increased stiffness, these dissipate somewhat more rapidly after completion of filling than in the previous case.

In the third case, in which self-desiccation is enabled, there is a significant increase in the degree of pore-pressure dissipation that takes place, indicating the potential importance of the self-desiccation mechanism in promoting dissipation of pore pressure. It should be noted that the dissipation of pore pressure would result in an increase the effective stress, which, in turn, promotes arching, resulting in a reduction in total vertical stress which would further reduce the pore pressure. The importance of this point will be illustrated later in the discussion on in situ measurements.

Influence of Permeability

To illustrate the influence of permeability on the overall filling response, analyses were carried out using the filling sequence and material properties described above, with C_c of 5%, but using three different permeability relationships [i.e., three different values of the permeability parameter c_k in Eq. (15)]. The resulting three permeability functions (denoted k_1, k_2, and k_3) are plotted against curing time in Fig. 11. In this plot, the change in k shown for each case is due only to cement growth, whereas in the cases modeled, the change could be significantly greater with the added effect of void-ratio reduction due to compression.

Fig. 12 shows the pore pressure during and following filling for a point 7 m above the base (i.e., 2 m above the lower-permeability "drawpoint" region) for the three cases considered. Fig. 13 shows the pore-pressure profile down through the stope at the end of filling. Also shown in Fig. 13 is the final steady-state pore pressure (SSPP) for the k_1 case, which is explained below (the SSPP lines for the other two cases are practically coincidental). In Fig. 12, the final steady-state equilibrium has been reached at about 230 h for the k_1 case, whereas changes were still occurring for the other two cases at this stage.

In Fig. 13, the line labeled k_1 SSPP refers to the SSPP that results from maintaining a water table in the stope at a 33.65-m height (the final filled height) and zero pore pressure at the base of the drawpoint, with the permeability in the lower 5 m being about 8 times less than the permeability in the stope proper for each case. Note that the permeability in the stope is not uniform with depth, so the ratio of 8 refers to average values. In Fig. 13, the difference between the pore pressure at the end of filling and the SSPP line indicates the excess pore pressure at this stage.

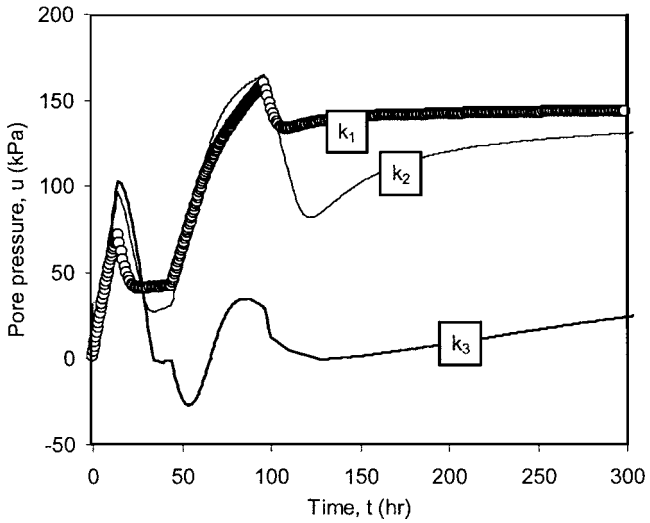

Fig. 12. Development of pore pressure for the three different permeability relationships shown in Fig. 11 (the total vertical stress for each case is identical to that shown in Fig. 10)

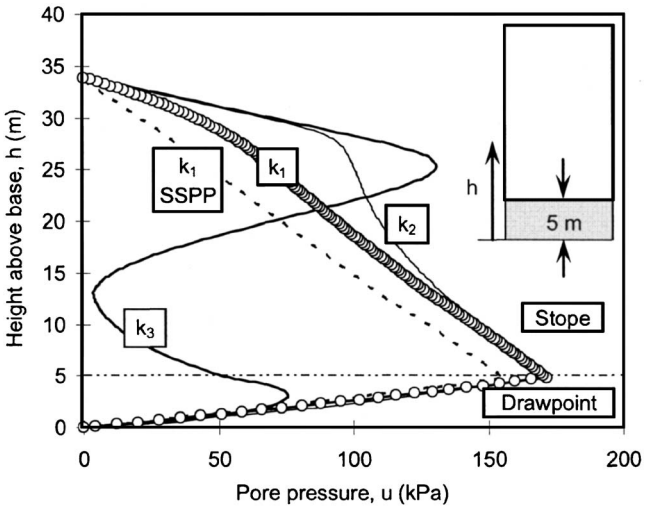

Fig. 13. Pore-pressure isochrones at the completion of filling for the three different permeability relationships shown in Fig. 11

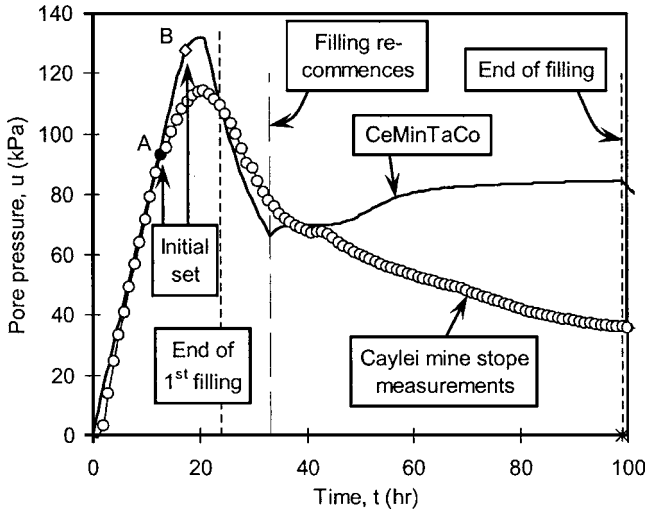

Fig. 14. Pore pressures measured in situ in a stope at the Caylei mine (Turkey), 1 m above the floor of the stope, compared with the output from the CeMinTaCo model

Thus, there are excess pore pressures in the stope for each of the three cases at the end of filling, but these are different for the three cases.

These results appear to be counterintuitive, since conventional consolidation theory suggests that high-permeability material should dissipate pore pressures more quickly than low-permeability material. Thus, in Fig. 12, while the lowest permeability case (k_3) shows the highest pore pressure in the first filling stage, it shows pore pressures very much *less* than the higher-permeability cases during the rest period and at all times thereafter. Examination of the pore-pressure plot at the end of filling for this case in Fig. 13 shows that from the surface down to about 25 m, the pore-pressure gradient corresponds to the total overburden stress gradient—i.e., there is no pore-pressure dissipation in this region at this stage—and, hence, the effective stresses are zero. However, below about 25 m, the pattern changes completely. In this region, hydration and self-desiccation are occurring, setting up high negative excess pore pressures. Though this results in a very steep downward hydraulic gradient (from 25 m down to 13 m), the low permeability prevents sufficient internal water flow from dissipating these negative pore pressures. If later, pore-pressure isochrones for this case were plotted, these would show the point of minimum pore pressure gradually moving upward until it reached the surface (as hydration progressed). Then, slow internal flows would gradually move the pore pressures onto the steady-state line.

For the highest permeability case (k_1), the same internal volume change occurs due to hydration, and, thus, the potential pore-pressure reduction resulting from this is the same. However, the higher permeability in this case means that high internal hydraulic gradients are not sustainable, due to the ease of generating internal water flow to smooth out the pore-pressure profile. Thus, at the end of filling, the pore pressures for the k_1 case are not very different from the SSPP values. Nevertheless, there is still evidence of the self-desiccation process occurring in this plot—i.e., the slight concave upward curvature of the pore-pressure profile from about 10–20 m would not be present if self-desiccation was not influencing the process. The intermediate permeability case (k_2) shows behavior similar to the k_1 case, commensurate with the fact that the permeability is not very much lower than for the k_1 case, as shown in Fig. 11.

Overall, this section has demonstrated that the behavior of cemented mine backfill during filling involves a complex interaction of mechanisms, and that the effect of self-desiccation can, in some circumstances, produce outcomes that are counterintuitive. For example, contrary to "rules of thumb" used in industry, filling a stope with low-permeability material with added cement can result in very low pore pressures being present in the fill at the end of filling—pore pressures much lower than those in a free-draining fill. Therefore, in order to predict the overall response, the individual mechanisms need to be incorporated into a fully coupled analysis, and this is what has been achieved in the CeMinTaCo program.

Comparison with Data from In Situ Monitoring of a Filled Stope

To determine how well the CeMinTaCo program can reproduce the behavior in an actual mine-backfilling situation, the program was used to simulate the deposition of a fine-grained cemented-paste fill at the Cayeli mine in Turkey. The properties of the as-placed material adopted in the modeling were in accordance with those in the field, including $e=1.0$, $C_c=8\%$, and q_u (after full hydration)$=1$ MPa. However, some of the other relevant material properties could not be determined directly, and thus, in order to gain a reasonable estimate of appropriate material properties, those determined for a similar tailings material with the same cement content were adopted. The values chosen in this way include the efficiency and rate of hydration ($E_h=0.032$, $d=1.5$), the ratio of q_u to $\Delta\sigma'_{vy}(=6)$, the uncemented compression parameters ($\lambda=0.06, \kappa=0.009$), permeability parameters ($k\approx 5\times 10^{-8}$ m/s), the ratio between cemented stiffness and strength (=1,300), and the damage coefficient ($b=0.5$). The method adopted to account for the flow restriction due to the drawpoint is the same as that used earlier in the parametric study (illustrated in Fig. 9).

The modeling was carried out by increasing the fill height at the same rate as in the field, i.e., a constant rate of rise of 0.4 m/h for the first 24 h followed by a 9-h rest period, and then filling the remainder of the stope at a rate of 0.4 m/h over a 100-h period. Fig. 14 shows a plot of pore pressure versus time obtained from

the modeling, compared to the field measurements. The monitoring location for the in situ measurements was 1.0 m above the stope floor, and the CeMinTaCo results plotted refer to the equivalent elevation.

In Fig. 14, the response during the initial stage of filling is linear (and, though not shown, coincides with the total stress increase during this period). However, the onset of initial set (point A for the measurements and point B for the model) coincides with a reduction in the rate of pore-pressure increase, such that from about 20 h onward, the pore-pressure is actually reducing for both the measured and model values even as filling continues (up to 24 h). When filling recommences (at approximately 33 h), the pore-pressure behavior appears to be reasonably well modeled initially, but as filling continues the model and in situ results diverge significantly. For the in situ case, it is likely that, due to consolidation, some of the fill/rock interface strength is mobilized, resulting in stress redistribution to the surrounding rock (arching). This reduces the total vertical stress imposed on the material at the monitoring point, resulting in a lower pore-pressure increase than would otherwise have occurred. In fact, any tendency for pore-pressure increase from this point onward is completely counteracted by ongoing drainage (and self-desiccation), with the result that the pore pressure at the monitoring point continues to reduce. Clearly, a one-dimensional model like CeMinTaCo model is not capable of accounting for the arching mechanism, and in this case it predicts an increase rather than a decrease in pore pressure when filling recommences.

While many of the material parameters used in the modeling have not been derived directly for the material being modeled, the ability of the model to reproduce the significant characteristic of the filling process based on properties of similar material illustrates that the model is capturing the most significant mechanisms associate with mine-fill placement. However, it is also clear that a two-dimensional model (plane strain or axisymmetric), or even a full 3D model, will be required to capture the complete behavior, and this is the subject of ongoing work.

Conclusion

This paper has outlined the basis of a numerical model for simulating the consolidation of cemented mine tailings. The work presented includes the development of a constitutive model, a permeability model and the concept of self-desiccation relative to the consolidation process. These have been implemented into a modified version of the MinTaCo program, called CeMinTaCo.

A sensitivity study (undertaken using typical mine-backfill parameters) indicated that both increasing stiffness and self-desiccation have a major influence on the consolidation process of cementing tailings. By varying the permeability it has been demonstrated that material with a higher permeability can actually develop higher pore pressures during filling than material of lower permeability. This seems counter to conventional consolidation theory and is a result of the interaction of different mechanisms, with self-desiccation having a major influence.

This sensitivity study also demonstrated that the various mechanisms associated with cemented mine-fill deposition can be highly interactive. As a result, treating the mechanism independently and superimposing their impact to determine the overall response can be misleading. Rather, at this stage, the only reasonable approach to understanding the mine-backfill process is through fully coupled numerical simulations using a program such as CeMinTaCo.

A comparison with in situ measurements indicates that during the early stages of fill placement, CeMinTaCo captures the relevant mechanisms very well. However, as time progresses, consolidation can result in some stress redistribution to the surrounding rock (arching) that reduces the total vertical stress. This mechanism cannot be captured using a one-dimensional program such as CeMinTaCo. To address this aspect, a two-dimensional model will be required, and this is the subject of ongoing development in this project.

Notation

The following symbols are used in this paper:

A = constant [Eq. (8)];
a_c = uncemented soil compression constant [Eq. (2)];
b = constant dictating the rate of cementation breakdown [Eq. (11)];
b_c = uncemented soil compression constant [Eq. (2)];
C_c = cement content: the weight of cement divided by the total dry weight;
d = constant that controls the rate of cementation development;
e = void ratio;
e_{eff} = effective void ratio when cement-gel growth is taken into account;
e_o = initial void ratio;
E'_o = constrained modulus of the soil skeleton;
E_h = efficiency of hydration, relating the total change in volume (in cm^3) that occurs as a result of the reaction of a given amount of cement (in g);
G_o = small strain-shear stiffness;
$G_{o(\text{inc})}$ = shear stiffness increment: Difference between the small strain-shear stiffness of a cemented soil and that for the uncemented soil under the same conditions;
k = material permeability;
K_w = bulk modulus of the water phase;
m = degree of cementation maturity (ranging from 0 to 1);
p' = Mean stress;
p'_a = stress level at which kinematic hardening occurs;
p'_c = applied effective stress;
p'_o = stress corresponding to uncemented normal consolidation at the current material state;
p'_y = isotropic yield stress;
q_u = unconfined compressive strength;
t = time;
t_o = time until initial cement set;
t^* = time after initial cement set ($=t-t_o$);
u = pore pressure;
w_c = weight of cement contained in each element;
X, Z, W = constant terms to relate the cemented strength to the material state [Eq. (8)];
α = kinematic hardening parameter;
Δe^p = plastic component of void-ratio change;
$\Delta p'_y$ = isotropic yield-stress increment;
$\Delta \sigma'_{vy}$ = incremental yield-stress in one-dimensional compression;
$\delta V_{\text{hyd}}/\delta t$ = rate of volume change due to self-desiccation;
Γ = void ratio at $p'=1$ kPa on the normal compression line for uncemented material;

γ_w = unit weight of water;
η = stress ratio (q/p');
κ = Cam-clay elastic compression constant;
λ = Cam-clay normal compression constant;
M = Cam-clay friction parameter;
σ'_v = effective vertical stress;
σ_v = total vertical stress; and
σ'_{vy} = effective vertical yield stress.

References

Carrier, W. D., III, Bromwell, L. G., and Somogyi, F. (1983). "Design capacity of slurried mineral waste ponds." *J. Geotech. Engrg.* 109, 699–716.

Carter, J. P., and Liu, M. D. (2005). Review of the structured cam clay model. *Soil Constitutive Models: Evaluation, Selection and Calibration*, ASCE, Geotechnical Special Publication No. 128, 99–132.

Consoli, N. C., Rotta, G. V., and Prietto, P. D. M. (2000). "Influence of curing under stress on the triaxial response of cemented soils." *Geotechnique* 50(1), 99–105.

Consoli, N. C., Rotta, G. V., and Prietto, P. D. M. (2006). "Yielding-compressibility-strength relationship for an artificially cemented soil cured under stress." *Geotechnique* 56(1), 69–72.

Dyvik, R., and Olsen, T. S. (1989). "G_{max} measured in oedometer and DSS tests using bender elements." *Proc., 12th Int. Conf. on SMFE*, International Society for Soil Mechanics and Foundation Engineering (ISSMFE), Rio de Janeiro, Vol. 1, Balkema, Rotterdam, The Netherlands, 39–42.

Fahey, M., and Newson, T. A. (1997). "Aspects of the geotechnics of mining wastes and tailings dams." *GeoEnvironment 97: Proc., 1st Australia—New Zealand Conf. on Environmental Geotechnics*, International Society for Soil Mechanics and Foundation Engineering (ISSMFE), Melbourne, Australia, 115–134.

Fahey, M., Newson, T. A., and Fujiyasu, Y. (2002). "Engineering with tailings." *Proc. 4th Int. Conf. on Environmental Geotechnics*, International Society for Soil Mechanics and Foundation Engineering (ISSMFE), Rio de Janeiro, Brazil, Vol. 2, 947–973.

Gibson, R. E., England, G. L., and Hussey, M. J. L. (1967). "The theory of one-dimensional consolidation of saturated clays. I: Finite nonlinear consolidation of thin homogenious layers." *Geotechnique*, 17(3), 261–273.

Helinski, M., Fourie, A. B., and Fahey, M. (2006). "Mechanics of early age cemented paste backfill." *Proc., 9th Int. Seminar on Paste and Thickened Tailings (Paste '06)*, R. Jewell, S. Lawson, and P. Newman eds., Limerick, Ireland, Australian Centre for Geomechanics, 313–322.

Helinski, M., Fourie, A. B., Fahey, M., and Ismail, M. (2007). "The self-desiccation process in cemented mine backfill." *Can. Geotech. J.* in press.

Illston, J. M., Dinwoodie, J. M., and Smith, A. A. (1979). *Concrete, Timber and Metals*, Van Nostrand Reinhold, New York.

Kuganathan, K. (2002). "A model to predict bulkhead pressures for safe design of bulkheads." *Filling with hydraulic fills*, Australian Centre for Geomechanics, Perth, Australia.

Le Roux, K. (2004). "In situ properties and liquefaction potential of cemented paste backfill." Ph.D. thesis, Univ. of Toronto, Canada.

Leroueil, S., and Vaughan, P. R. (1990). "The general and congruent effects of structure in natural soils and weak rocks." *Geotechnique* 40(3), 467–488.

Li, L., and Aubertin, M. (2003) "A general relationship between porosity and uniaxial strength of engineering materials." *Can. J. Civ. Eng.*, 30, 644–658.

Liu, M. D., and Carter, J. P. (2002). "A structured Cam Clay model." *Can. Geotech. J.*, 39, 1313–1332.

Liu, M. D., Carter, M. D., Desaim, C. S., and Xu, K. J. (1998). "Analysis of the compression of structured soils using the disturbed state concept." *Report No. R770*, Dept. of Civil Engineering, Univ. of Sydney, Sydney, NSW, Australia.

Powers, T. C., and Brownyard, T. L. (1947). "Studies of the physical properties of hardened Portland cement paste." *Bull. No. 22*, Research Laboratory of Portland Cement Association, Skokie, Ill. [reprinted from *J. Am. Concr. Inst. (Proc.)*, Vol. 43 (1947)].

Rankin, R. (2004). "Geotechnical characterization and stability of paste fill stopes at Cannington mine." Ph.D. thesis, James Cook Univ., Townsville, Queensland, Australia.

Rastrup, E. (1956). "The temperature function for heat of hydration in concrete." *Proc., RELIM Symposium: Winter Concreting, Theory, and Practice*, Session B(II), Danish Institute for Building Research, Copenhagen.

Rotta, G. V., Consoli, N. C., Prietto, P. D. M., Coop, M. R., and Graham, J. (2003). "Isotropic yielding in an artificially cemented soil cured under stress." *Geotechnique* 53(5), 493–501.

Seneviratne, N., Fahey, M., Newson, T. A., and Fujiyasu, Y. (1996). "Numerical modeling of consolidation and evaporation of slurried mine tailings." *Int. J. Numer. Analyt. Meth. Geomech.*, 20(9), 647–671.